FULL PAPER

Dalton

www.rsc.org/dalton

Triangles and tetrahedra: metal directed self-assembly of metallo-supramolecular structures incorporating bis-β-diketonato ligands†

Jack K. Clegg,[a] Leonard F. Lindoy,[a] Boujema Moubaraki,[b] Keith S. Murray[b] and John C. McMurtrie[a]

[a] *Centre for Heavy Metals Research, School of Chemistry, University of Sydney, NSW, 2006, Australia*

[b] *Department of Chemistry, Monash University, PO Box 23, VIC, 3800, Australia*

Received 11th March 2004, Accepted 21st June 2004
First published as an Advance Article on the web 19th July 2004

The interaction of six aryl-linked bis-β-diketones, including a new naphthylene linked species, with copper(II), iron(III) and, in one instance gallium(III), has been investigated with the aim of obtaining metallo-supramolecular assemblies exhibiting different geometries. New examples of two assembly types incorporating the above bis-β-diketones (L) were generated. The first type is represented by a range of molecular triangles of formula $[Cu_3(L–H_2)_3](solvent)_n$ while the second is given by a corresponding selection of less-common neutral molecular tetrahedra of formula $[Fe_4(L–H_2)_6](solvent)_n$ as well as $[Ga_4(L–H_2)_6]\cdot 8.5THF\cdot 0.5H_2O$; an example of each type has been characterised by X-ray crystallography. A magnetochemical investigation of $[Fe_4(\mathbf{3}–H_2)_6]\cdot 6THF$ is reported. The susceptibility is Curie like and consistent with very weak coupling occurring between the iron(III) d^5 (high spin) centres. The X-ray structures of two trinuclear copper(II) as well as a tetranuclear iron(III) and a tetranuclear gallium(III) assembly confirm their discrete triangular and tetrahedral geometries, respectively. The structure of the gallium(III) species is closely related to that of the corresponding iron(III) species. The tetrahedral structures provide rare examples of such assemblies encapsulating guest solvent molecules – in each case tetrahydrofuran is incorporated in the central cavity.

Introduction

The design and synthesis of new molecular assemblies incorporating transition metal ions as structural elements has received very considerable attention over recent years.[1] The presence of transition metals in such systems yields the potential for exhibiting additional functionality; the latter includes unusual optical, magnetic, photoactive, catalytic and/or electrochemical properties. Additionally, for many systems the metal plays the dual role of directing the course of the self-assembly process towards the required metallo-supramolecular product. For example, the use of a tetrahedral metal ion instead of an octahedral one has been demonstrated to have a marked effect on the formation of metal-containing helical structures.[2] In now classical studies, when tetrahedral copper(I) was reacted with a linked poly(bipyridyl) ligand containing flexible spacers between the individual bipyridyl groups then a double helix was generated.[3] In contrast, the use of an octahedral metal (such as high-spin nickel(II)) in an analogous study employing a closely related ligand system yielded a triple helix.[4]

Besides helices, there have now been many reports[5] of metallo-supramolecular assemblies exhibiting a wide range of molecular architectures whose shape is dictated by the metal directing properties of a given metal ion coupled with the steric requirements of an appropriate ligand component or components. Examples include triangles,[6] squares,[7] tetrahedra,[8] capsules,[9] and other higher polyhedral shapes.[10] While great diversity of structure occurs for metallo-supramolecular systems, in general, less variation is apparent when the ligand components used for their construction are considered. For example, di- or oligo-bipyridyl or phenanthroline derivatives have been common metal-coordination motifs employed for the production of many metallo-systems. In contrast, derivatives of some other common ligand categories, for example, the β-diketones, have received much less attention.[11] The metal coordination abilities of simple β-diketones have been investigated since Alfred Werner's time[12] and such ligands have been well documented to be versatile metal coordinating agents;[13] further, they can be readily synthesised in a variety of derivative forms.[14,15] In the present investigation we have employed bis-β-diketone derivatives of types **1**–**6** to construct new molecular triangles and tetrahedra. Given the allowable orientations of the chelating groups in these potentially bifunctional ligands, the latter are clearly structurally capable of acting as the 'sides' of molecular triangles (in which square-planar divalent metal ions occupy the corners) or as the edges of molecular tetrahedra (incorporating octahedral metal ions at the corners).

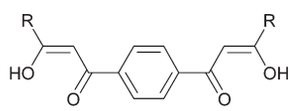

1; R = Me
2; R = Et
3; R = Pr
4; R = t-Bu
5; R = Ph

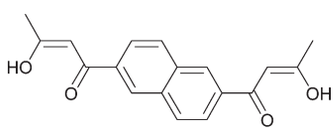

6

In prior studies, mixed-donor analogues of the above ligands of type **7** have been employed for the construction of triangular complexes of type $[M_3(L–H_2)_3]$ (M = Ni or Cu) with an X-ray structure determination confirming the trinuclear nature of the species with M = Ni (low-spin).[16] In further studies, linked dialkyl malonates such as **8**, which also share many of the characteristics of bis-β-diketones,[17] undergo interaction with octahedral iron(III) on deprotonation to yield neutral, tetrahedral-shaped assemblies of formula $[Fe_4(L–H_2)_6]$.[18] We now report the synthesis and investigation of a

† Electronic supplementary information (ESI) available: Tables S1–S4: selected bond lengths (Å) and angles (°) for the crystallographically characterised complexes. Fig. S1: Crystal packing diagram of $[Cu_3(\mathbf{1}–H_2)_3(DMF)]\cdot DMF$. Fig. S2: Crystal lattice of $[Cu_3(\mathbf{3}–H_2)_3]\cdot 0.3MeCN$ viewed parallel to the *a* axis. Fig. S3: ORTEP representation of the asymmetric unit of $[Ga_4(\mathbf{1}–H_2)_6]\cdot 8.5THF\cdot 0.5H_2O$. See http://www.rsc.org/suppdata/dt/b4/b403673e/

DOI: 10.1039/b403673e

new series of triangle- and tetrahedron-shaped metallo-assemblies incorporating the doubly deprotonated forms of the β-diketone derived ligands **1**–**6**.

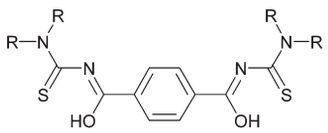

7

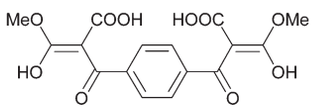

8

Experimental

All reagents and solvents were purchased from commercial sources and used without further purification unless otherwise stated. ^{1}H NMR spectra were recorded on a Bruker Avance DPX200 spectrometer; δ_H values are relative to Me_4Si; low resolution, positive ion electrospray ionisation mass spectra (ESI-MS) were obtained on a Finnigan LCQ-8 spectrometer in methanol–tetrahydrofuran; in no case were parent ions observed for the respective metal-containing products. FTIR (KBr) spectra were collected using a Bio-Rad FTS-40 spectrometer. UV-VIS spectra were recorded on a Cary 1E spectrophotometer; in all cases the visible region contained the 'tail' of an intense charge transfer and/or ligand absorption that extended from the UV region. Solid-state X-band EPR spectra were obtained on powdered samples at room temperature as the first derivatives on a Bruker EMX EPR spectrometer (operating microwave frequency ~9.3 GHz) equipped with a Bruker EMX 081 magnet and an ERO 41XG microwave bridge. Magnetic susceptibility data were collected using a Quantum Design MPMS SQUID magnetometer under an applied field of 1 T.

The syntheses of **1**–**6** involved Claisen condensations using an adaptation of literature procedures.[14,19] To a mixture of dimethyl terephthalate (5 g, 0.025 mol) (for **1**–**5**), dimethyl naphthalene-2,6-dicarboxylate (6.1 g, 0.025 mol) (for **6**) and acetone (2.9 g, 0.05 mol) (for **1** and **6**), butan-2-one (3.6 g, 0.05 mol) (for **2**), pentan-2-one (4.3 g, 0.05 mol) (for **3**), 3,3-dimethylbutan-2-one (5 g, 0.05 mol) (for **4**), acetophenone (6 g, 0.05 mol) (for **5**) in dry diethyl ether (80 ml) was added sodium amide (5 g, 0.13 mol) at 273 K. In each case the mixture was stirred for 2 h at 273 K and then 2 h at 298 K over which time the reaction mixture became yellow. The reaction was then quenched with iced water (100 ml). Any insoluble material was filtered off and the aqueous layer was acidified with CO_2(s) to yield an off-white precipitate. The precipitate was collected in each case. The ether layer was evaporated and the off-white residue was combined with the above precipitate before recrystallisation from methanol.

1,1′-(1,4-Phenylene)bisbutane-1,3-dione, 1

Yield 3.11 g (50%) of yellow needles. Anal. Calc. for $C_{14}H_{14}O_4$: C, 68.28; H, 5.73%. Found: C, 68.03; H, 5.74%. ^{1}H NMR ($CDCl_3$): δ 16.00 (br s, enol, 2H), 7.98 (s, C_6H_4, 4H), 6.21 (s, CH enol, 2H), 2.23 (s, CH_3, 6H). ESI-MS: *m*/*z* 247 ($M + H^+$). FTIR (KBr): 3000(br), 1600(vbr), 1281(br), 1117, 1081, 1019, 779 cm^{-1}.

1,1′-(1,4-Phenylene)bispentane-1,3-dione, 2

Yield 2.8 g (41%) of light brown needles. Anal. Calc. for $C_{16}H_{18}O_4$: C, 70.06; H, 6.61%. Found: C, 69.76; H, 6.67%. ^{1}H NMR ($CDCl_3$): δ 16.04 (br s, enol, 2H), 7.97 (s, C_6H_4, 4H), 6.25 (s, CH enol, 2H), 2.54 (q, CH_2, 4H), 1.26 (t, CH_3, 6H). ESI-MS: *m*/*z* 275 ($M + H^+$), 297 ($M + Na^+$). FTIR (KBr): 3000(br), 1600(vbr), 1507, 1292, 1161, 1118, 1055, 858, 812, 775 cm^{-1}.

1,1′-(1,4-Phenylene)bishexane-1,3-dione, 3

Yield 3.0 g (40%) of light brown plates. Anal. Calc. for $C_{18}H_{22}O_4$: C, 71.50; H, 7.33%. Found: C, 71.35; H, 7.38%. ^{1}H NMR ($CDCl_3$): δ 16.01 (br s, enol, 2H), 7.87 (s, C_6H_4, 4H), 6.13 (s, –CH– enol, 2H), 2.37 (t, $–CH_2–$, 4H), 1.65 (q, $–CH_2–$, 4H), 0.94 (t, $–CH_3$, 6H). ESI-MS: *m*/*z* 303 ($M + H^+$), 325 ($M + Na^+$). FTIR (KBr): 3000(br), 1600(vbr), 1559, 1506, 1465, 1437, 1363, 1301, 1263, 1162, 1119, 1073, 951, 857, 784 cm^{-1}.

1,1′-(1,4-Phenylene)bis-3,3-dimethylpentane-1,3-dione, 4

Yield 3.4 g (41%) of light yellow plates. Anal. Calc. for $C_{20}H_{26}O_4$: C, 72.70; H, 7.93%. Found: C, 72.43; H, 8.06%. ^{1}H NMR ($CDCl_3$): δ 16.5 (br s, enol, 2H), 7.95 (s, C_6H_4, 4H), 6.34 (s, CH enol, 2H), 1.26 (s, $–CH_3$, 18H). ESI-MS: *m*/*z* 331 ($M + H^+$), 353 ($M + Na^+$). FTIR (KBr): 2980(br), 1600(vbr), 1559, 1507, 1437, 1397, 1362, 1221, 1114, 1081, 781 cm^{-1}.

1,1′-(1,4-Phenylene)bis-3-phenylpropane-1,3-dione, 5

Yield 3.2 g (36%) of pale yellow crystalline powder. Anal. Calc. for $C_{24}H_{18}O_4$: C, 77.82; H, 4.90%. Found: C, 77.80; H, 5.07%. ^{1}H NMR ($CDCl_3$): δ 16.83 (br s, enol, 2H), 8.10 (s, C_6H_4, 4H), 8.04–7.54 (m, Ph, 10H), 6.91 (s, CH enol, 2H). ESI-MS: *m*/*z* 371 ($M + H^+$), 393 ($M + Na^+$). FTIR (KBr): 2800(br), 1680(vbr), 1525, 1489, 1306, 1234, 1069, 926, 854, 798, 753, 681 cm^{-1}.

1,1′-(2,6-Naphthylene)bisbutane-1,3-dione, 6

Yield 3.5 g (37%) of pale yellow crystalline powder. Anal. Calc. for $C_{18}H_{16}O_4 \cdot 0.45H_2O$: C, 71.00; H, 5.59%. Found: C, 70.98; H, 5.58%. ^{1}H NMR ($CDCl_3$): δ 16.15 (br s, enol, 2H), 8.45 (s, arom, 2H), 7.97 (m, arom, 4H), 6.33 (s, CH enol, 2H), 2.26 (s, CH_3, 6H). ESI-MS: *m*/*z* 297 ($M + H^+$), 319 ($M + Na^+$). FTIR (KBr): 2900(br), 1696, 1600(br), 1427, 1366, 1340, 1296, 1188, 1138, 915, 773, 487, 472 cm^{-1}.

Synthesis of complexes of type $[Cu_3(L–H_2)_3]$ and $[M_4(L–H_2)_6]$ (M = Fe, Ga). The required ligand (0.002 mol) (chosen from **1**–**6**) in dry THF (40 ml) was added to $NaHCO_3$, (1.0 g, 0.008 mol), or Na_2CO_3 (1.0 g, 0.01 mol) in dry THF (10 ml). The mixture was stirred for 1 h before copper(II) chloride dihydrate (0.002 mol) (for the trinuclear systems), or anhydrous iron(III) or gallium(III) chloride (0.0013 mol) (for the tetranuclear systems) dissolved in dry THF (40 ml) was added dropwise. The mixture was stirred for a further 2 h for the copper(II) complexes or 16 h for the iron(III) and gallium(III) complexes, then filtered and the filtrate collected. The solution was either allowed to evaporate slowly to yield the solid complex which was isolated by filtration or the solvent was removed on a rotary evaporator and the crude solid obtained was recrystallised from THF. All products were washed with methanol before analysis.

$[Cu_3(1–H_2)_3]\cdot 3H_2O\cdot 1.5THF$

Yield 0.54 g (75%), green microcrystalline powder. Anal. Calc. for $C_{42}H_{36}Cu_3O_{12}\cdot 3H_2O\cdot 1.5THF$: C, 53.18; H, 5.02%. Found: C, 52.93; H, 5.43%. VIS (solid state): ~460 sh, ~700 (vbr) nm; [THF solution (molar extinction/dm^3 mol^{-1} cm^{-1})]: ~460 sh, ~650 (vbr) (275) nm. Crystals of $[Cu_3(\mathbf{1}–H_2)_3(DMF)]\cdot DMF$ suitable for X-ray analysis were obtained in the following manner. Copper(II) acetate monohydrate (0.001 mol) in DMF (100 ml) was added dropwise to **1** (0.001 mol) in refluxing DMF (100 ml). The mixture was stirred for 1 h then left to evaporate slowly at room temperature over several months whereupon the product crystallised as olive green crystals.

$[Cu_3(2–H_2)_3]$

Yield 0.49 g (73%), green microcrystalline powder. Anal. Calc. for $C_{48}H_{48}Cu_3O_{12}$: C, 57.22; H, 4.80%. Found: C, 57.32; H, 5.11%. VIS (solid state): ~460 sh, ~700 (vbr) nm.

$[Cu_3(3–H_2)_3]\cdot 2H_2O$

Yield 0.56 g (75%), green microcrystalline powder. Anal. Calc. for $C_{54}H_{60}Cu_3O_{12}\cdot 2H_2O$: C, 57.58; H, 5.73%. Found: C, 57.73; H, 5.65%. VIS (solid state): ~450 sh, ~560 (br), ~660 sh (vbr) nm. Olive green hexagonal crystals of $[Cu_3(\mathbf{3}–H_2)_3]\cdot 0.3MeCN$ suitable for X-ray analysis were grown by slow evaporation of a 50% acetonitrile–THF solution of the complex over two days.

$[Cu_3(6–H_2)_3]\cdot 4THF\cdot 6H_2O$

Yield 0.60 g (61%), green microcrystalline powder. Anal. Calc. for $C_{54}H_{42}Cu_3O_{12}\cdot 4THF\cdot 6H_2O$: C, 57.24; H, 5.91%. Found: C, 57.44; H, 6.24%. VIS (solid state): ~460 sh, ~720 (vbr) nm.

$[Fe_4(1–H_2)_6]\cdot 12H_2O\cdot 2THF$

Yield 0.60 g (76%), red crystals. Anal. Calc. for $C_{84}H_{72}Fe_4O_{24}\cdot 12H_2O\cdot 2THF$: C, 53.89; H, 5.51%. Found: C, 53.78; H, 5.83%. VIS (solid state): 500 br (sh) nm.

$[Fe_4(2–H_2)_6]\cdot H_2O$

Yield 0.54 g (79%), red crystals. Anal. Calc. for $C_{96}H_{96}Fe_4O_{24}\cdot H_2O$: C, 61.46; H, 5.27%. Found: C, 61.06; H, 5.58%. VIS (solid state): ~500 sh (br) nm. Prismatic crystals suitable for X-ray analysis were obtained by slow evaporation of the reaction solution.

$[Fe_4(3–H_2)_6]\cdot 6THF$

Yield 0.54 g (75%), red crystals. Anal. Calc. for $C_{108}H_{96}Fe_4O_{24}\cdot 6THF$: C, 64.47; H, 6.89%. Found: C, 64.46; H, 6.99%. VIS (solid state): ~480 sh (br) nm. [THF solution]: ~480 sh (br) nm. Prismatic crystals suitable for X-ray analysis were obtained by slow evaporation of the reaction solution.

$[Fe_4(4–H_2)_6]\cdot 3THF$

Yield 0.59 g (76%), red crystals. Anal. Calc. for $C_{120}H_{144}Fe_4O_{24}\cdot 3THF$: C, 65.78; H, 7.03%. Found: C, 66.46; H, 6.94%. VIS (solid state): ~490 sh (br) nm.

$[Fe_4(5–H_2)_6]\cdot H_2O\cdot 10THF$

Yield 0.55 g (61%), red crystals. Anal. Calc. for $C_{120}H_{144}Fe_4O_{24}\cdot H_2O\cdot 10THF$: C, 66.17; H, 6.62%. Found: C, 65.95; H, 5.02%. VIS (solid state): ~540 sh (vbr), nm.

$[Fe_4(6–H_2)_6]\cdot 5THF\cdot 7H_2O$

Yield 0.55 g (67%), red microcrystalline powder. Anal. Calc. for $C_{108}H_{84}Fe_6O_{24}\cdot 5THF\cdot 7H_2O$: C, 62.07; H, 5.62%. Found: C, 61.93; H, 5.99%. VIS (solid state): ~570 sh (vbr) nm.

$[Ga_4(1–H_2)_6]\cdot 8.5THF\cdot 0.5H_2O$

Orange crystals of this product, suitable for X-ray analysis, were isolated from the corresponding THF reaction solution. The crystals lost solvent very rapidly (within seconds) after removal from the mother-liquor. One of these crystals was cooled and used directly for the X-ray study. ^{1}H NMR (DMSO-d_6): δ 7.92 (m, arom, 16H), 7.66 (s, arom, CH, 8H), 6.5 (m, CH, 8H), 6.1 (s, 4H), 2.23 (m, CH_3, 36H). No further characterisation of this product was attempted.

X-Ray structure determinations

Data were collected at 150(2) K with ω scans to approximately 56° 2θ using a Bruker SMART 1000 diffractometer employing graphite-monochromated Mo-Kα radiation generated from a sealed tube (0.71073 Å). Data integration and reduction were undertaken with SAINT and XPREP[20] and subsequent computations were carried out using the WinGX-32 graphical user interface.[21] Multi-scan empirical absorption corrections were applied to the data using the program SADABS.[22] Gaussian absorption corrections were applied using XPREP.[20] Structures were solved by direct methods using SIR97[23] then refined and extended with SHELXL-97.[24] Unless otherwise stated, ordered non-hydrogen atoms were refined anisotropically while partial occupancy non-hydrogen atoms were refined isotropically. Hydrogen atoms attached to carbon atoms were included in idealised positions and a riding model was used for their refinement.

Crystal and structure refinement data

The refinement residuals are defined as $R1 = \Sigma||F_o| - |F_c||/\Sigma|F_o|$ for $F_o > 2\sigma(F_o)$ and $wR2 = \{\Sigma[w(F_o^2 - F_c^2)^2]/\Sigma[w(F_c^2)^2]\}^{1/2}$ where $w = 1/[\sigma^2(F_o^2) + (AP)^2 + BP]$, $P = (F_o^2 + 2F_c^2)/3$ and A and B are listed with the crystal data for each structure.

$[Cu_3(1–H_2)_3(DMF)]\cdot DMF$. Formula $C_{48}H_{50}Cu_3N_2O_{14}$, $M = 1069.52$, triclinic, space group $P\bar{1}$ (#2), $a = 7.580(1)$, $b = 16.588(2)$, $c = 18.967(3)$ Å, $\alpha = 104.282(2)$, $\beta = 92.545(2)$, $\gamma = 93.097(2)$, $V = 2303.7(6)$ Å^3, $D_c = 1.542$ g cm^{-3}, $Z = 2$, crystal size 0.35 × 0.12 × 0.05 mm, colour green, habit prism, temperature 150(2) K, λ(Mo-Kα) = 0.71073, μ(Mo-Kα) 1.443 mm^{-1}, T(empirical)$_{min,max}$ = 0.781, 0.930, $2\theta_{max} = 56.9$, *hkl* range −10 to 10, −22 to 22, −24 to 25, $N = 22074$, $N_{ind} = 10614$ ($R_{merge} = 0.0267$), $N_{obs} = 7860$ ($I > 2\sigma(I)$), $N_{var} = 583$, residuals $R1(F, 2\sigma) = 0.0440$, $wR2(F^2$, all) = 0.1182, $A = 0.060$, $B = 1.8193$, GoF(all) = 1.016, $\Delta\rho_{min,max} = -0.982$, 1.330 e$^-$ Å^{-3}.

Individual details. The DMF solvate molecule is orientationally disordered and was modelled with two overlapping positions (occupancies 0.65 and 0.35).

$[Cu_3(3–H_2)_3]\cdot 0.3MeCN$. Formula $C_{54.6}H_{60.9}Cu_3N_{0.3}O_{12}$, $M = 1103.96$, hexagonal, space group $P6_3$ (#173), $a = b = 21.2843(17)$, $c = 13.616(2)$ Å, $V = 5342.0(11)$ Å^3, $D_c = 1.373$ g cm^{-3}, $Z = 4$, crystal size 0.50 × 0.50 × 0.40 mm, colour green, habit hexagonal pyramid, temperature 150(2) K, λ(Mo-Kα) = 0.71073, μ(Mo-Kα) 1.243 mm^{-1}, T(empirical)$_{min,max}$ = 0.533, 0.610, $2\theta_{max} = 57.0$, *hkl* range −27 to 28, −28 to 28, −17 to 17, $N = 53479$, $N_{ind} = 8748$ ($R_{merge} = 0.0293$), $N_{obs} = 7723$ ($I > 2\sigma(I)$), $N_{var} = 420$, residuals $R1(F, 2\sigma) = 0.0434$, $wR2(F^2$, all) = 0.1235, $A = 0.082$, $B = 2.6212$, GoF(all) = 1.045, $\Delta\rho_{min,max} = -0.804$, 1.296 e$^-$ Å^{-3}.

Individual details. the lattice contains two structurally independent but conformationally similar trinuclear copper complexes, both of which have crystallographic 3-fold symmetry. The terminal ethyl component of one of the structurally independent complexes was disordered over two positions and was modelled accordingly (atom positions C(1a)–C(2a), occupancy 0.65 and C(1b)–C(2b), occupancy 0.35). The occupancy of the MeCN molecule, which also lies on a 3-fold axis, refined to *ca.* 0.2 and was fixed at this value for the final refinement cycles. There is no crystallographic relationship between the two complexes in the asymmetric unit indicating that the correct space group symmetry is non-centrosymmetric (chiral) $P6_3$ and not the related centrosymmetric space group $P6_3/m$. The Flack[25] parameter refined to 0.120(13) indicating that the crystal was a racemic twin with a major twin fraction of approximately 0.9.

$[Fe_4(3–H_2)_6]\cdot 6THF$. Formula $C_{132}H_{168}Fe_4O_{30}$, $M = 2458.06$, tetragonal, space group $I4_1/a$ (#88), $a = b = 28.866(4)$, $c = 17.326(5)$ Å, $V = 14437(5)$ Å^3, $D_c = 1.131$ g cm^{-3}, $Z = 4$, crystal size 0.47 × 0.31 × 0.11 mm, colour red, habit prism, temperature 150(2) K, λ(Mo-Kα) = 0.71073, μ(Mo-Kα) 0.930 mm^{-1}, T(Gaussian)$_{min,max}$ = 0.774, 0.955, $2\theta_{max} = 56.6$, *hkl* range −38 to 36, −38 to 38, −22 to 13, $N = 47576$, $N_{ind} = 8688$ ($R_{merge} = 0.0599$), $N_{obs} = 4912$ ($I > 2\sigma(I)$), $N_{var} = 324$, residuals $R1(F, 2\sigma) = 0.0877$, $wR2(F^2$, all) = 0.2659, $A = 0.15$, $B = 0.00$, GoF(all) = 1.130, $\Delta\rho_{min,max} = -1.039$, 1.592 e$^-$ Å^{-3}.

Individual details. The asymmetric unit contains one quarter of the molecule which is located near a $\bar{4}$ special position. The ethyl

groups comprising atoms C(1)–C(2) and C(19)–C(20) were disordered over two sites and were modelled accordingly. The entire propyl group comprising atoms C(16)–C(18) displays more extensive conformational disorder and was modelled in two orientations. The terminal methyl group of one of these orientations was further disordered over three sites. Bond length and angle restraints were applied to all disordered groups. The central cavity of the complex contained significant electron density that was modelled as a single THF molecule with overlapping 4-fold disorder around the central $\bar{4}$ special position. The difference Fourier map also showed two regions of smeared electron density surrounding the complex. Once these were modelled as positionally disordered THF (four sites, total occupancy one), rigid group refinement was used for all THF molecules and thermal parameters were modelled with U_{iso} values fixed at 0.06. The second region of electron density (located near a $\bar{4}$ site) could not be effectively modelled. The SQUEEZE function of PLATON[26,27] was employed to remove this contribution of electron density from the intensity data. By symmetry, there are four such regions in the unit cell. PLATON estimated the electron count to be 47 for each and since there are 40 electrons per THF this, therefore, corresponds reasonably closely to one THF molecule per region. By elemental analysis, the proposed formula is $[Fe_4(\mathbf{3}–H_2)_6]\cdot 6THF$ which is also in agreement with the crystal structure.

$[Ga_4(\mathbf{1}–H_2)_6]\cdot 8.5THF\cdot 0.5H_2O$. Formula $C_{118}H_{141}Ga_4O_{33}$, $M = 2366.19$, monoclinic, space group $C2/c$ (#15), $a = 28.037(5)$, $b = 16.944(3)$, $c = 27.090(5)$ Å, $\beta = 104.840(3)°$, $V = 12440(4)$ Å^3, $D_c = 1.263$ g cm^{-3}, $Z = 4$, crystal size 0.41 × 0.10 × 0.09 mm, colour orange, habit plate, temperature 150(2) K, λ(Mo-Kα) = 0.71073, μ(Mo-Kα) 0.930 mm^{-1}, T(empirical)$_{min,max}$ = 0.663, 0.916, $2\theta_{max} = 56.3$, hkl range −37 to 35, −15 to 22, −35 to 35, $N = 39988$, $N_{ind} = 14462$ ($R_{merge} = 0.0957$), $N_{obs} = 6516$ ($I > 2\sigma(I)$), $N_{var} = 686$, residuals $R1(F, 2\sigma) = 0.0773$, $wR2(F^2$, all) = 0.2062, $A = 0.06$, $B = 0.00$, GoF(all) = 1.285, $\Delta\rho_{min,max} = -0.663$, 1.91 e$^-$ Å^{-3}.

Individual details. The crystals of this complex decomposed into powder almost instantly after removal from the mother-liquor and as such they were handled and mounted at *ca.* 200 K prior to quenching in the cryostream at 150 K. The tetranuclear complex has 2-fold crystallographic symmetry and as such the asymmetric unit contains half of the total metal complex. The asymmetric unit also contains three full occupancy THF molecules, two half occupancy THF molecules, one THF with occupancy 0.25 (located in the central cavity of the tetranuclear complex) and one water molecule (occupancy 0.25).

CCDC reference numbers 233534–233536 and 235189.

See http://www.rsc.org/suppdata/dt/b4/b403673e/ for crystallographic data in CIF or other electronic format.

Results and discussion

In the present study trinuclear copper(II) complexes of type $[Cu_3L_3]\cdot(solvent)_n$ (where L is the doubly deprotonated forms of **1**–**3** and **6**) while, with iron(III), tetranuclear species of type $[Fe_4L_6]\cdot(solvent)_n$, (where L is the doubly deprotonated forms of **1**–**6**) were synthesised. It is the presence of sp^2 hybridisation throughout the backbones of these dianionic ligands, coupled with the presence of appropriately substituted 'spacer' groups, that aids the formation of the target triangular and tetrahedral geometries mentioned previously. All complexes were characterised by elemental microanalysis, UV-vis spectroscopy, and in a number of cases, by single crystal X-ray crystallography. A single gallium(III) complex with the formula $[Ga(\mathbf{1}–H_2]\cdot 8.5THF\cdot 0.5H_2O$ was also isolated and characterised by X-ray crystallography.

In earlier studies of the complexation behaviour of **1** and **5** in their dianionic forms,[28,29] it was postulated that the complexes of these ligands with four-coordinate divalent metal ions exist as polymeric species and a recent X-ray study by Soldatov *et al.* confirmed the polymeric nature of the pyridine adduct of the zinc(II) complex of dianionic **5**–H$_2$.[30] The latter workers also demonstrated that **5**–H$_2$ forms discrete trimeric species of type $[M_3(\mathbf{5}–H_2)_3(pyridine)_3]\cdot n CHCl_3$ with cobalt(II) and nickel(II). X-Ray studies demonstrate that each of these metal species has a similar trigonal structure in which the metals are in a triangular arrangement, with the pyridine ligands occupying axial positions on each metal centre.

In an attempt to circumvent possible polymer formation in the present study, complexes were synthesised by the slow addition of a solution of the appropriate metal salt to a solution of the ligand in the presence of sodium carbonate or hydrogencarbonate as base. Any precipitate and remaining base were filtered off and the product then recovered from the filtrate.

Copper(II) triangles

Copper species of type $[Cu_3L_3]\cdot(solvent)_n$ were synthesised by reaction of a 1 : 1 ratio of ligand to copper(II) chloride in THF in the presence of excess solid sodium carbonate or hydrogencarbonate as base. The solid-state VIS spectra of the copper(II) complexes are listed in the Experimental section. All spectra consist of a broad envelope of d–d bands in the visible region together with the 'tail' from more intense peaks in the UV region corresponding to charge transfer/ligand bands. The spectra are quite similar to those reported previously for 'simple' β-diketone complexes of type [Cu(β-diketonato)$_2$].[31] The solution (THF) spectrum of $[Cu_3(\mathbf{1}–H_2)_3]\cdot 3H_2O\cdot 1.5THF$ is similar in broad detail to its corresponding solid-state spectrum. However, due to the broadness of the spectra, speculation concerning the solution structure of the product based on this appears inappropriate.

The X-ray structure of $[Cu_3(\mathbf{1}–H_2)_3(DMF)]\cdot DMF$ was determined. This discrete trinuclear complex, illustrated in Fig. 1, has three copper(II) ions occupying the corners of an equilateral triangle and three dianionic (**1**–H$_2$) ligands comprising the sides. The structure is essentially planar, although, the chelate rings and phenyl groups deviate slightly from the mean plane of the molecule. The molecule incorporates six delocalised six-membered chelate rings. Cu(2) and Cu(3) have approximately square-planar coordination geometries, but interestingly, Cu(1) has square-based pyramidal geometry due to coordination of a DMF molecule. While Cu(I) is unambiguously five-coordinate, both Cu(2) and Cu(3) may be considered to have pseudo-six-coordinate geometries with each of these copper(II) ions lying directly above and below an electron rich area of another molecule, either a β-diketonato chelate ring or a phenyl group. These possible 'contact' distances range from 2.8 to 3.5 Å.

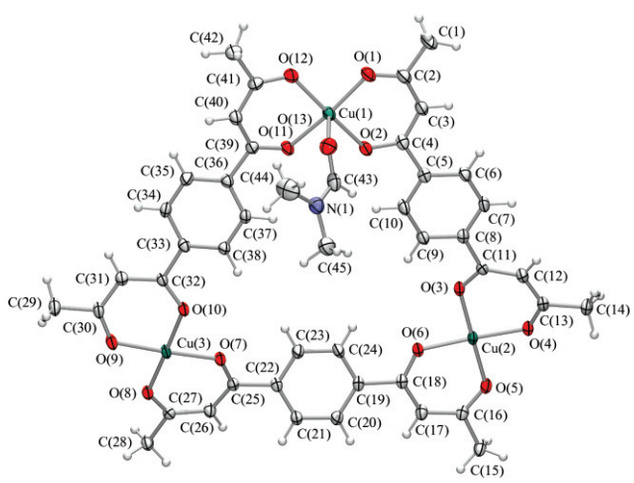

Fig. 1 ORTEP representation of $[Cu_3(\mathbf{1}–H_2)_3(DMF)]\cdot DMF$ with thermal ellipsoids drawn at the 50% probability level. The DMF solvate molecule has been omitted for clarity.

In the crystal lattice (Fig. S1, ESI†) the complexes are arranged in columns parallel to the crystallographic *a* axis. The molecules of adjacent columns intercalate to form the apparent Cu···π interactions mentioned above. These intercalated molecules stack into two-dimensional sheets parallel to the *ac* plane; the ligands in the vicinity of the five-coordinate copper(II) ion coordinated to the DMF do

not intercalate. Adjacent sheets are separated by disordered DMF solvate molecules.

The crystal structure of $[Cu_3(\mathbf{3}–H_2)_3]\cdot 0.3MeCN$, illustrated in Fig. 2, shows many similarities to that of $[Cu_3(\mathbf{1}–H_2)_3(DMF)]\cdot DMF$, particularly in terms of the geometry adopted by the ligands and the nature of the interactions of the metals with adjacent chelate or phenyl rings. The complex is again a discrete equilateral-triangular species. As expected, the geometry adopted is once again clearly a reflection of the inherent steric properties of both the copper(II) ion and its ligands. The structure differs from that of $[Cu_3(\mathbf{1}–H_2)_3(DMF)]\cdot DMF$ in that no solvent molecule is bound to a metal centre, but rather, disordered acetonitrile is incorporated (see below) in the centre of the triangular structure. The $[Cu_3(\mathbf{3}–H_2)_3]\cdot 0.3MeCN$ lattice contains two crystallographically independent, but structurally similar trinuclear copper complexes, both of which have crystallographic 3-fold symmetry. One of the complexes encircles the acetonitrile solvate, while the other is solvent free. The complexes are arranged in layers that stack with a separation of approximately 3 Å along the crystallographic *c* axis (Fig. S2, ESI†). While the formal coordination number of each copper(II) ion is four, as before, there are possible intermolecular interactions between the copper(II) sites and the electron-rich areas of adjacent molecules, with contact distances ranging from 2.8 to 3.2 Å. The individual molecules are arranged in two structurally different columns, one with a circular channel and one with a triangular channel (which encloses the acetonitrile solvate). The molecules in adjacent columns overlap to produce the apparent axial Cu(II)–π contacts. The EPR spectrum of the above trinuclear complex was determined on a frozen THF solution at 150 K. Quantitative assignment of the spectrum was hampered by the complexity of the signals; however, consistent with the crystallographic data, the spectrum clearly shows the presence of more than one species with axial or/and lower symmetry. The absence of significant copper nuclei interaction is also suggested by the absence of a low intensity multiplet at lower field, which is due to forbidden half-field transitions ($\Delta M_S = \pm 2$).

Iron(III) tetrahedra

As mentioned already, complexes of type $[Fe_4L_6]\cdot(solvent)_n$ were synthesised for all six of the present ligand systems. These were obtained by reaction of iron(III) chloride and ligand in THF in a 2 : 3 ratio.

The crystal structure of $[Fe_4(\mathbf{3}–H_2)_6]\cdot 6THF$ was determined and an ORTEP representation of the asymmetric unit is shown in Fig. 3. The crystal symmetry is tetragonal (space group $I4_1/a$) and the molecule is situated around a $\bar{4}$ special position. The asymmetric unit therefore consists of one quarter of the molecule. The complete molecular structure is illustrated in Figs. 4 and 5. This tetranuclear assembly has the expected pseudo-tetrahedral stereochemistry with the four iron(III) ions situated at the vertices of the tetrahedron and the six ligands bridging the metal ions defining the edges. Each iron(III) is six-coordinate with approximate octahedral coordination geometry.

As in the structures of $[Cu_3(\mathbf{1}–H_2)_3(DMF)]\cdot DMF$ and $[Cu_3(\mathbf{3}–H_2)_3]\cdot 0.3MeCN$, the ligands are twisted and the chelate rings belonging to each ligand are not co-planar; in part, this undoubtedly reflects the need for the iron(III) ions to attain an approximate octahedral geometry. The molecule is host to a THF guest. The structure represents a less common example of a neutral tetrahedral cage complex. The encapsulation of a neutral guest molecule within such a system is even more uncommon. Attempts to investigate this complex further by ^{1}H NMR in DMSO-d_6 and acetone-d_6 were unsuccessful due to extensive contact shift broadening of the signals due to the presence of the paramagnetic iron(III) ions. The similarity between the solid and solution phase VIS spectra, however, suggests that the iron(III) chromophore observed in the solid state may be maintained in solution. The volume of the solvent-accessible void within the assembly was estimated using PLATON[26] to be 25 Å^3. The semi-schematic view of the molecular structure (Fig. 5) emphasises its tetrahedral shape and also illustrates the presence of open faces.

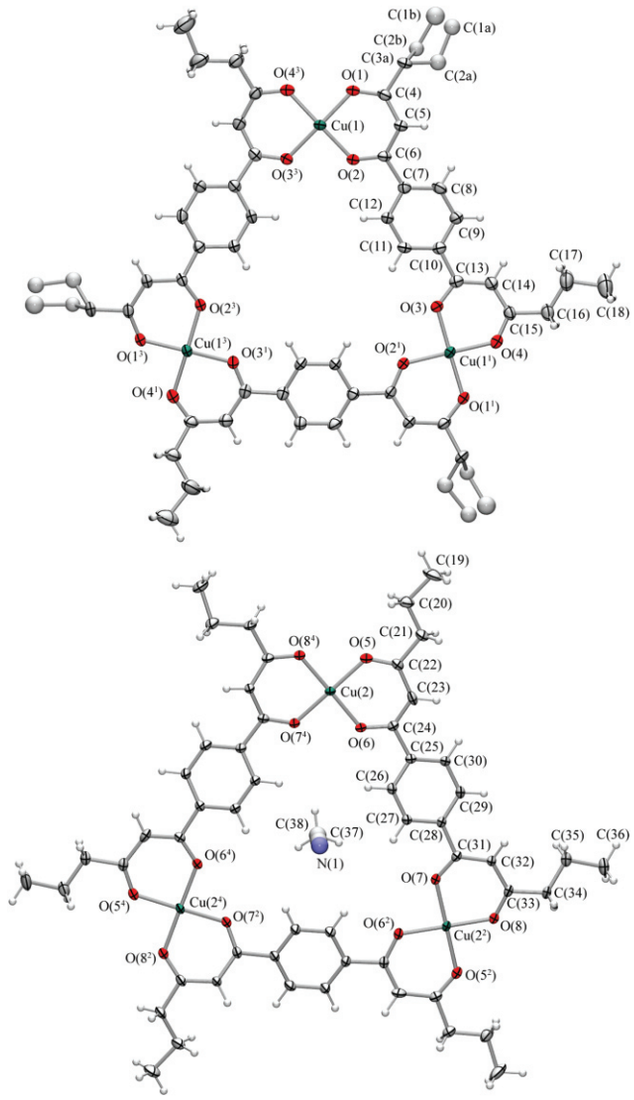

Fig. 2 ORTEP representations of the symmetry independent complexes in the lattice of $[Cu_3(\mathbf{3}–H_2)_3]\cdot 0.3MeCN$ (shown with 50% probability ellipsoids). The two crystallographically independent complexes both have 3-fold symmetry. The interior space of one of these (bottom) contains an acetonitrile molecule while the other is solvent free (top). Symmetry codes: $^1 -x+y+2, -x+1, z$; $^2 -y+1, x-y, z$; $^3 -y+1, x-y-1, z$; $^4 -x+y+1, -x+1, z$.

A crude crystal structure of the related complex $[Fe_4(\mathbf{2}–H_2)_6]\cdot H_2O$, recrystallised from THF, was also determined and this species was again shown to be tetranuclear with a similar tetrahedral arrangement of the iron atoms to that found for $[Fe_4(\mathbf{3}–H_2)_6]\cdot 6THF$. However, details of this structure are not presented here as its refinement was problematic due to the presence of extensive twinning and poor crystal quality.

A magnetochemical investigation of $[Fe_4(\mathbf{3}–H_2)_6]\cdot 6THF$ was undertaken. Plots of reciprocal magnetic susceptibility and magnetic moment, per cluster, are given as a function of temperature in Fig. 6. The susceptibility is Curie like and thus indicative of very weak coupling between the iron(III) d^5 (high spin) centres in the cluster. This can be seen in the magnetic moment behaviour in which the moment remains independent of temperature down to ~20 K, with a value of 11.82 μ_B (5.91 μ_B per iron(III)) which is essentially the spin-only moment for these four high-spin d^5 ions. The sharp decrease below 20 K is probably due to zero-field splitting of the $^6A_{1g}$ single ion iron(III) centres, but may indicate some very weak antiferromagnetic coupling. Such behaviour is expected for bis-β-diketonate bridging ligands, which will provide poor superexchange pathways for spin–spin coupling between the metal ions within the tetranuclear cluster. A combination of long Fe–Fe distances and weak delocalisation *via* the aromatic spacer is reflected by the weak exchange coupling observed. It is noted that related ligands such

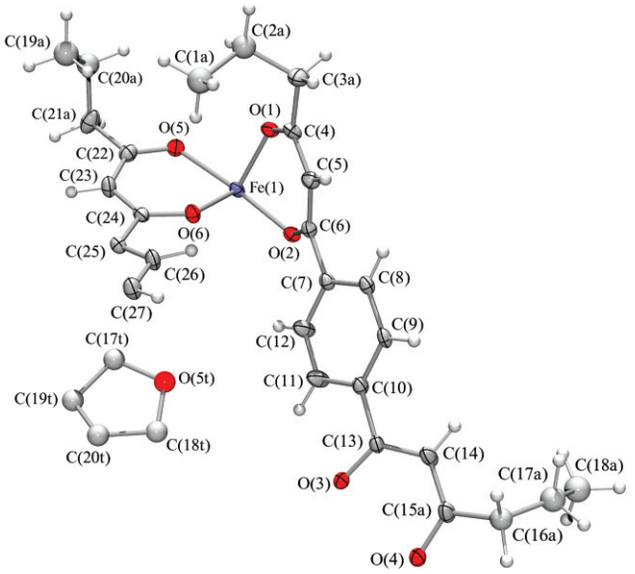

Fig. 3 ORTEP representation of the asymmetric unit of $[Fe_4(\mathbf{3}–H_2)_6]\cdot 6THF$ with ellipsoids drawn at the 25% probability level. Only the highest occupancy position is shown for each disordered component. The THF guest molecule is also included in the diagram but THF solvate has been omitted for clarity.

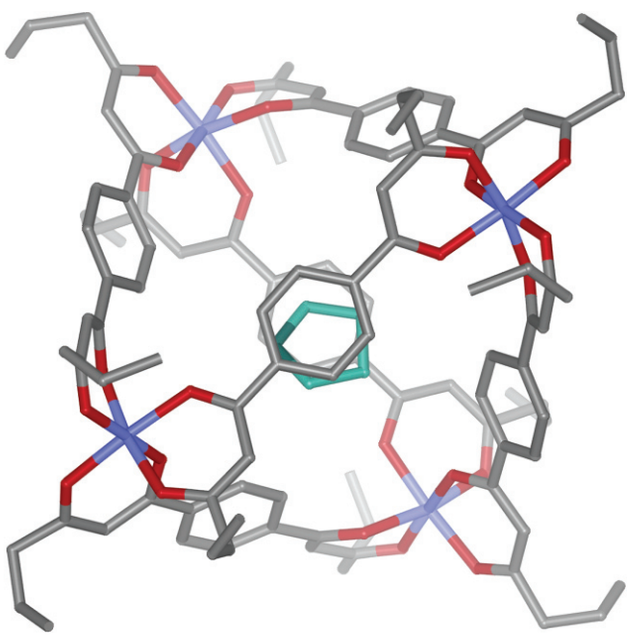

Fig. 4 The molecular structure of the tetrahedral $[Fe_4(\mathbf{3}–H_2)_6]$ metallo-supramolecular assembly viewed along the S_4 axis (Cu blue, O red, C grey). The THF guest molecule is also shown (green).

as 1,4-dicarboxybenzene (terephthalate) also give weak coupling, the metals being closer with this bridging ligand compared to the present ligand.[32]

A gallium(III) tetrahedron

Using a similar procedure to that employed for the iron(III) complexes in which gallium(III) chloride was substituted for iron(III) chloride led to the isolation of the crystalline complex $[Ga_4(\mathbf{1}–H_2)_6]\cdot 8.5THF\cdot 0.5H_2O$ for which the crystal structure was obtained (an ORTEP depiction of the structure along with geometrical details are provided as ESI†). The tetranuclear structure is again similar to that of $[Fe_4(\mathbf{3}–H_2)_6]\cdot 6THF$, with the gallium atoms defining a tetrahedron and the central cavity showing partial occupancy of a THF molecule. The ^1H NMR spectra of this product in DMSO-d_6 and acetone-d_6 was considerably more complex than that of the free ligand showing the presence of three –CH= environments in each case as well as multiplets in the aromatic region.

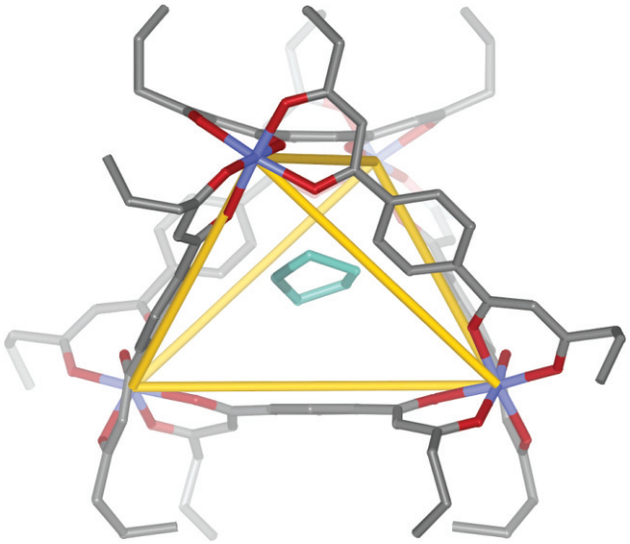

Fig. 5 The structure of $[Fe_4(\mathbf{3}–H_2)_6]$ viewed normal to the S_4 axis. The yellow connectors drawn between Fe(III) centres (blue) highlight the tetrahedral shape of the molecule which encapsulates a THF guest (green). The ligands form the tetrahedral edges leaving the tetrahedral faces open.

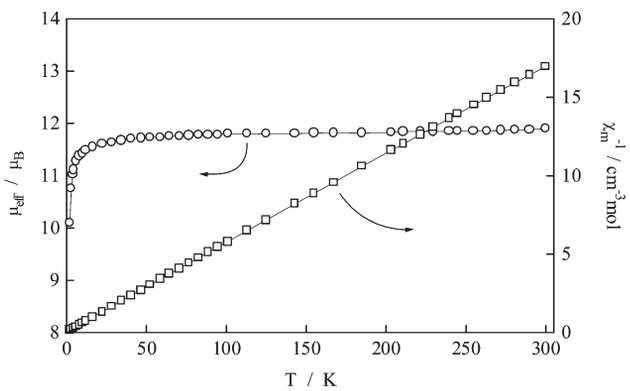

Fig. 6 The reciprocal magnetic moment and magnetic susceptibility *vs.* temperature per molecule of $[Fe_4(\mathbf{3}–H_2)_6]\cdot 6THF$.

While the spectra might be interpreted as showing that a unsymmetric structure is maintained in solution (as observed by X-ray diffraction for the solid state), it is also consistent with at least partial dissociation of the structure occuring in DMSO-d_6 under the conditions employed. Because of the overall complexity of the spectra, this aspect was not pursued further.

Concluding remarks

The present study reports the complexation behaviour of **1**–**6** with copper(II), iron(III) and gallium(III) to yield, in all, eleven metallo-supramolecular assemblies. Apart from their intrinsic interest, the achievement of such an extended range of new triangular and tetrahedral metallo-supramolecular structures serves to illustrate the facility with which such species assemble under defined conditions, despite the use of ligand systems incorporating a range of substituent types.

Acknowledgements

We thank the Australian Research Council for support and Dr M. Fainerman-Melnikova for undertaking the EPR study.

References

1 L. F. Lindoy and I. M. Atkinson, *Self-Assembly in Supramolecular Systems*, Monographs in Supramolecular Chemistry, Royal Society of Chemistry, Cambridge, UK, 2000.
2 See, for example: J.-M. Lehn and A. Rigault, *Angew. Chem., Int. Ed. Engl.*, 1988, **27**, 1095; J.-M. Lehn, T. M. Garrett, U. Koert, J.-M. Lehn, A. Rigault, D. Meyer and J. Fischer, *J. Chem. Soc., Chem. Commun.*,

1990, 557; M. Harding, U. Koert, J.-M. Lehn, A. Marquis-Rigault, C. Piguet and J. Siegel, *Helv. Chim. Acta.*, 1991, **74**, 594; N. Kimizuka, S. Fujkikawa, H. Kuwahara, T. Kunitake, A. Marsh and J.-M. Lehn, *J. Chem. Soc., Chem. Commun.*, 1995, 2103; B. Hasenknopf, J.-M. Lehn, B. O. Kneisel, G. Baum and D. Fenske, *Angew. Chem., Int. Ed. Engl.*, 1996, **35**, 1838; L. A. Cuccia, J.-M. Lehn, J.-C. Homo and M. Schmutz, *Angew. Chem., Int. Ed.*, 2000, **39**, 233; M. Albrecht, *Chem. Rev.*, 2001, **101**, 3457; R. W. Saalfrank, I. Bernt, F. Hampel., A. Scheurer, T. Nakajima, S. H. Z. Huma, F. W. Heinemann, M. Schmidtmann and A. Muller, *Polyhedron*, 2003, **22**, 2985.

3 J.-M. Lehn, A. Rigault, J. Siegel, J. Harrowfield, B. Chevrier and D. Moras, *Proc. Natl. Acad. Sci. USA*, 1987, **84**, 2565.

4 R. Krämer, J.-M. Lehn, A. De Cian and J. Fischer, *Angew. Chem., Int. Ed. Engl.*, 1993, **32**, 703.

5 J.-M. Lehn, *Supramolecular Chemistry: Concepts and Perspectives*, VCH, Weinheim, 1995; M. Fujita and K. Ogura, *Coord. Chem. Rev.*, 1996, **148**, 249; S. Leininger, B. Olenyuk and P. J. Stang, *Chem. Rev.*, 2000, **100**, 853; F. Hof, S. Craig, C. Nuckolls and J. Rebek, Jr., *Angew. Chem., Int. Ed.*, 2002, **41**, 1488.

6 R.-D. Schnebeck, L. Randaccio, E. Zangrando and B. Lippert, *Angew. Chem., Int. Ed.*, 1998, **37**, 119; R.-D. Schnebeck, E. Freisinger, F. Glahé and G. Lippert, *J. Am. Chem. Soc.*, 2000, **122**, 1381; R. W. Saalfrank, N. Low, B. Demleitner, D. Stalke and M. Teichert, *Chem. Eur. J.*, 1998, **4**, 1305.

7 P. Teo, L. L. Koh and T. S. A. Hor, *Inorg. Chem.*, 2003, **42**, 7290.

8 R. W. Saalfrank, R. Burak, A. Breit, D. Sstalke, R. Herbst-Irmer, J. Daub, M. Porsch, E. Bill, M. Müther and A. Trautwien, *Angew. Chem., Int. Ed. Engl.*, 1994, **33**, 1621; N. Takeda, K. Umemoto, K. Yamaguchi and M. Fujita, *Nature*, 1999, **398**, 794; T. Beissel, R. E. Powers and K. N. Raymond, *Angew. Chem., Int. Ed. Engl.*, 1996, **35**, 1084; D. Caulder and K. Raymond, *J. Chem. Soc., Dalton Trans*, 1999, 1185; T. Beissel, R. E. Powers, T. N. Parac and K. N. Raymond, *J. Am. Chem. Soc.*, 1999, **121**, 4200; S. K. Umemoto, K. Yamaguchi and M. Fujita, *J. Am. Chem. Soc.*, 2000, **122**, 7150; C. He, L. Wang, Z. Wang, Y. Liu, C. Liao and C. Yan, *J. Chem. Soc., Dalton Trans.*, 2002, 134.

9 B. Olenyuk, M. D. Levin, J. A. Whiteford, J. E. Shield and P. J. Stang, *J. Am. Chem. Soc.*, 1999, **121**, 10434; B. F. Abrahams, S. J. Egan and R. Robson, *J. Am. Chem. Soc.*, 1999, **121**, 3535; S. R. Seidel and P. J. Stang, *Acc. Chem. Res.*, 2002, **35**, 972; J.-P. Lang, Q.-F. Xu, Z.-N. Chen and B. F. Abrahams, *J. Am. Chem. Soc.*, 2003, **125**, 12682.

10 N. Takeda, K. Umemoto, K. Yamaguchi and M. Fujita, *Nature*, 1999, **398**, 794; B. Olenyuk, M. D. Levin, J. A. Whiteford, J. E. Shield and P. J. Stang, *J. Am. Chem. Soc.*, 1999, **121**, 10434; B. Olenyuk, J. A. Whiteford, A. Fechtenkötter and P. J. Stang, *Nature*, 1999, **398**, 796; F. A. Cotton, L. M. Daniels, C. Lin and C. A. Murillo, *Chem. Commun.*, 1999, 841; F. A. Cotton, C. Lin and C. A. Murillo, *Inorg. Chem.*, 2001, **40**, 6413; F. A. Cotton, C. Lin and C. A. Murillo, *Acc. Chem. Res.*, 2001, **34**, 759; M. Eddaoudi, J. Kim, J. B. Wachter, H. K. Chae, M. O'Keeffe and O. M. Yaghi, *J. Am, Chem. Soc.*, 2001, **123**, 4368; B. Moulton, J. Lu, A. Mondalk and M. J. Zaworotko, *Chem. Commun.*, 2001, 863; D. K. Chand, K. Biradha, M. Fujita, S. Sakamoto and K. Yamaguchi, *Chem. Commun.*, 2002, 2486.

11 S. Wang, H. L. Tsai, W. E. Streib, G. Christou and D. N. Hendrickson, *J. Chem. Soc., Chem. Commun.*, 1992, 1427; M. A. Halcrow, J. C. Huffman and G. Christou, *Angew. Chem., Int. Ed. Engl.*, 1995, **34**, 889; V. A. Grillo, E. J. Seddon, C. M. Grant, G. Aromi, J. C. Bollinger, K. Folting and G. Christou, *Chem. Commun.*, 1997, 1561.

12 A. Werner, *Ber. Dtsch. Chem. Ges.*, 1901, **34**, 2594.

13 A. G. Swallow and M. R. Truter, *Proc. R. Soc. London, Ser. A*, 1960, **254**, 205; D. Gibson, *Coord. Chem. Rev.*, 1969, **4**, 225; F. P. Dwyer and D. P. Mellor, *Chelating Agents and Metal Chelates*, Academic Press, London, 1964; U. Casellato, P. Vigato and M. Vivaldi, *Coord. Chem. Rev.*, 1977, **23**, 31; U. Casellato, *Chem. Soc. Rev.*, 1979, **8**, 199.

14 D. Martin, M. Shamma and W. Fernelius, *J. Am. Chem. Soc.*, 1958, **80**, 4891.

15 A. W. Maverick and F. E. Klavetter, *Inorg. Chem.*, 1984, **23**, 4130; G. Aromi, P. Gamez, P. Berzal, C. Paula, W. L. Driessen and J. Reedijk, *Synth. Commun.*, 2003, **33**, 11, and references therein.

16 R. Köhler, R. Kirmse, R. Richter, J. Sieler and E. Hoyer, *Z. Anorg. Allg. Chem.*, 1985, 537.

17 R. W. Saalfrank, A. Starkj, K. Peters and H. von Schnerin, *Angew. Chem., Int. Ed. Engl.*, 1988, **27**, 851; R. W. Saalfrank, B. Hörner, D. Stalke and J. Salbeck, *Angew. Chem., Int. Ed. Engl.*, 1993, **32**, 1179.

18 R. W. Saalfrank, R. Burak, S. Reihs, N. Löw, F. Hampel, H. Stachel, J. Lentmaier, K. Peters, E. Peters and H. von Schnering, *Angew. Chem., Int. Ed. Engl.*, 1995, **34**, 993.

19 D. J. Gosciniak and N. J. Patrick, Ultraviolet radiation absorbing compositions of bis-1,3-diketone derivatives of benzene, *Eur. Pat. Appl.*, EP 0 376 511 A2, 1990.

20 Bruker; SMART, SAINT and XPREP: Area detector control and data integration and reduction software, Bruker Analytical X-Ray Instruments Inc. Madison, WI, USA, 1995.

21 WinGX-32: System of Programs for solving, refining and analysing single crystal X-ray diffraction data for small molecules; L. J. Farrugia, *J. Appl. Crystallogr.*, 1999, **32**, 837.

22 G. M. Sheldrick, SADABS: Empirical absorption and correction software, University of Göttingen, Institüt für Anorganische Chemie der Universität, Tammanstrasse 4, D-3400 Göttingen, Germany, 1999.

23 A. Altomare, M. C. Burla, M. Camalli, G. L. Cascarano, C. Giocavazzo, A. Guagliardi, A. G. C. Moliterni, G. Polidori and S. Spagna, *J. Appl. Crystallogr.*, 1999, **32**, 115.

24 G. M. Sheldrick, SHELX-97: Programs for crystal structure analysis, University of Göttingen, Institüt für Anorganische Chemie der Universität, Tammanstrasse 4, D-3400 Göttingen, Germany, 1998.

25 H. D. Flack, *Acta Crystallogr., Sect. A*, 1983, **39**, 876.

26 A. L. Spek, *Acta Crystallogr., Sect. A*, 1990, **46**, C34.

27 P. van der Sluis and A. L. Spek, *Acta Crystallogr., Sect. A*, 1990, **46**, 194.

28 D. E. Fenton, C. M. Regan, U. Casellato, P. A. Vigato and M. Vivaldi, *Inorg. Chim. Acta*, 1982, **58**, 83.

29 M. M. Matsushita, T. Yasuda, R. Kawano, T. Kawai and T. Iyoda, *Chem. Lett.*, 2000, **7**, 812.

30 D. V. Soldatov, A. S. Zanina, G. D. Enright, C. I. Ratcliffe and J. A. Ripmeester, *Cryst. Growth Des.*, 2003, **3**, 1005.

31 R. L. Belford, M. Calvin and G. Bedford, *J. Chem. Phys.*, 1957, **26**, 1165.

32 See for example: Y.-T. Li, C.-W. Yan, Y.-F. Lu and D.-Z. Liao, *Transition Met. Chem.*, 1998, **23**, 237.